Novel retinylidene iminium salts for defining opsin shifts: synthesis and intrinsic chromophoric properties

Michael Åxman Petersen,[a] Iben B. Nielsen,[b] Michael B. Kristensen,[b] Anders Kadziola,[a] Lutz Lammich,[b] Lars H. Andersen*[b] and Mogens Brøndsted Nielsen*[a]

Received 5th January 2006, Accepted 17th February 2006
First published as an Advance Article on the web 13th March 2006
DOI: 10.1039/b600121a

Retinal Schiff bases serve as chromophores in many photoactive proteins that carry out functions such as signalling and light-induced ion translocation. The retinal Schiff base can be found as neutral or protonated, as all-*trans*, 11-*cis* or 13-*cis* isomers and can adopt different conformations in the protein binding pocket. Here we present the synthesis and characterisation of isomeric retinylidene iminium salts as mimics blocked towards isomerisation at the C11 position and conformationally restrained. The intrinsic chromophoric properties are elucidated by gas phase absorption studies. These studies reveal a small blue-shift in the $S_0 \rightarrow S_1$ absorption for the 11-locked derivative as compared to the unlocked one. The gas phase absorption spectra of all the cationic mimics so far investigated show almost no absorption in the blue region. This observation stresses the importance of protein interactions for colour tuning, which allows the human eye to perceive blue light.

Introduction

Many photoactive proteins that perform visual signalling and light-induced ion translocation contain the retinal chromophore.[1–5] Thus, all vertebrate visual pigments are integral-membrane proteins containing a protonated Schiff base of 11-*cis*-retinal at the seventh α-helix of opsin. Vertebrates have two kinds of photoreceptor cells, called cones and rods. Cones function in bright light and are responsible for colour vision, whereas rod cells function in dim light but do not perceive colour. The primary event in visual excitation is isomerisation of the 11-*cis*-retinal to all-*trans*-retinal, which leads to significant changes in the geometry and to significant strain in the protein. After a series of conformational changes, the imine is deprotonated, and all-*trans*-retinal is eventually liberated through a hydrolysis step.[5] Bacteriorhodopsin, present in the purple membrane of *Halobacterium salinarum*,[6] contains a protonated Schiff base of all-*trans*-retinal. This protein is responsible for transmembrane proton-pumping,[7] a process that is fuelled by light-induced 13-*trans*→13-*cis* isomerisation.

Our ability to distinguish colours relies on a fascinating tuning of the chromophore absorption maximum *via* subtle protein interactions.[1,2,5] Absorption data are usually compared to those of protonated retinal Schiff bases in methanol solution where the absorption maximum is at about 440 nm for both *cis*- and *trans*-configurations of the chromophore.[8] The shift in absorption maximum from this value as experienced by a protein is termed 'the opsin shift'.[9] Rhodopsin present in rods exhibits an absorption maximum at *ca.* 500 nm, *i.e.* an opsin shift of 60 nm, whereas proteins present in human cone pigments absorb with a maximum somewhere in the region between ~420 and ~560 nm.[2,5] Bacteriorhodopsin shows a maximum at 570 nm.[7] Moreover, the cascade of conformational changes occurring after light-induced isomerisation of both bacteriorhodopsin and rhodopsin provides a series of conformers each of which experiences a unique absorption maximum.[5,10]

We have recently determined experimentally the gas phase absorption spectra of all-*trans* retinal derivatives **1** and **2** (Fig. 1) in the protonated or methylated Schiff base form, respectively (*cationic mimics*).[11] We used a technique where photo-absorption was registered by detection of photo-fragments. Briefly, the

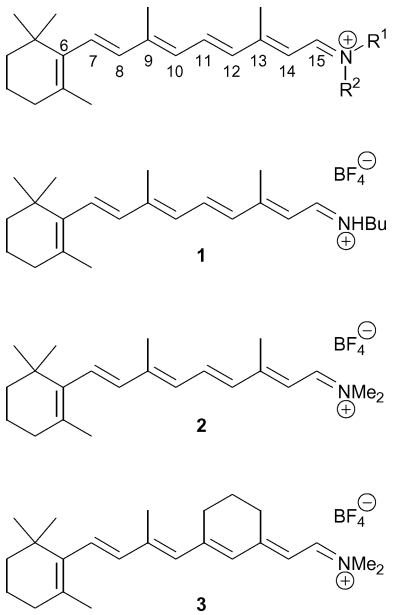

Fig. 1 Compounds **1** and **2** are mimics of the protonated retinal Schiff base present in proteins (R^1 = lysine side chain and R^2 = H). The 11-locked derivative **3** presents a new target molecule for the investigation of intrinsic chromophoric properties.

[a]*Department of Chemistry, University of Copenhagen, Universitetsparken 5, DK-2100, Copenhagen Ø, Denmark. E-mail: mbn@kiku.dk*
[b]*Department of Physics and Astronomy, University of Aarhus, DK-8000, Aarhus C, Denmark. E-mail: lha@phys.au.dk*

chromophore molecules were transferred to the gas phase by electrospray ionisation and injected into an electrostatic ion storage ring where they were irradiated by a tuneable, pulsed laser.[12] On account of the increased energy (typically 2 eV) after absorption of a single photon, the microcanonical temperature of the chromophore ions was increased by several hundreds of Kelvin and spontaneous Arrhenius-type fragmentation happened over a time scale of about a millisecond.[13] The storage-ring technique enabled us to keep excited chromophores and wait for delayed decays to occur. Upon spontaneous fragmentation, neutral photo-fragments were not kept stored by the storage ring, but were detected on a dedicated particle detector, the signals of which made up the absorption spectrum, after normalisation to the number of photons in the laser pulse and the number of ions in the storage ring. The method allows investigation of charged molecules that cannot be studied in the gas phase by simple evaporation. Moreover, absorption data of isolated chromophores in the gas phase are highly desirable for a number of reasons: Firstly, they provide the best reference for quantum chemical calculations. Secondly, for protonated chromophores like protonated Schiff base retinal, there is always a negative counter ion in the solutions which may not easily be controlled. Thirdly, a series of studies have indeed suggested that the conditions inside many photo-active proteins like the Green Fluorescent Protein are almost vacuum like.[14]

To shed further light on the intrinsic chromophoric properties of cationic Schiff bases of retinal and any possible differences between isomers as well as conformers, we decided to lock the C11 double bond towards isomerisation. Since the absorption behaviour of compounds **1** and **2** is very similar,[11] the methylated iminium derivative **3** was chosen as the next target compound rather than a protonated one. A locked chromophore may naturally have slightly different vibrational properties which may be displayed in the electronic absorption spectrum.

Results and discussion

Synthesis

The synthesis of isomeric 11-locked retinylidene iminium salts starts from ketones **4** (all-*E*) and (9*Z*)-**4** (Scheme 1).[15] The conversion of these ketones into immediate precursors for the iminium salts follows a synthetic protocol previously reported by Albeck *et al.*,[15] but in contrast to this protocol we isolated all intermediate isomers by careful chromatographic separation when possible in order to subject each isomer to individual transformations. For simplicity, we shall only specify the positions of *Z*-configuration in the compound labeling. Isomer designations were performed by a combination of ^{1}H NMR spectroscopy and X-ray crystallographic analyses (*vide infra*).

First, the ketone **4** was subjected to an Emmons–Horner reaction with diethyl cyanomethylphosphonate to afford the two nitriles **5** and (13*Z*)-**5** (Scheme 1). These two isomers were separated by careful column chromatographic work-up. Similarly, the ketone (9*Z*)-**4** was transformed into nitriles (9*Z*)-**5** and (9*Z*,13*Z*)-**5**.

Reduction of **5** with diisobutyl aluminiumhydride (DIBALH) provided the aldehyde **6** that was subsequently treated with dimethylammonium tetrafluoroborate to provide the new iminium

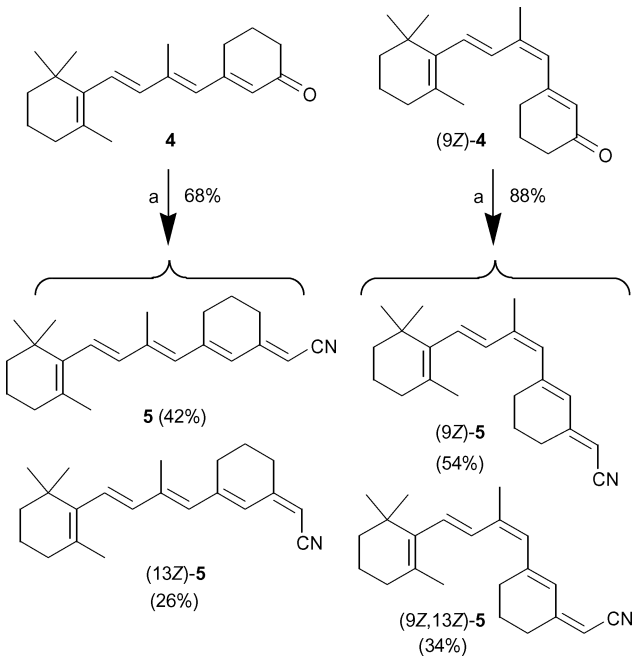

Scheme 1 *Reagents and conditions*: (a) $(EtO)_2POCH_2CN$, NaH, THF, rt.

salt **3** together with the (13*Z*)-**3** isomer in a ratio of 9 : 1 (Scheme 2). These iminium salt isomers were impossible to separate. Reduction of nitrile (13*Z*)-**5** gave aldehyde (13*Z*)-**6** that, however, under chromatographic work-up partly isomerised to the all-*E* isomer **6**. Further isomerisation occurred during reaction with dimethylammonium tetrafluoroborate to provide a mixture of (13*Z*)-**3** and **3** in favour of the all-*E* salt. The (13*Z*)-**3** : **3** ratio of 1 : 8 is close to that obtained (1 : 9) when starting from the all-*E* aldehyde **6**. Reduction of (9*Z*)-**5** gave almost isomerically pure aldehyde (9*Z*)-**6**. However, treatment with dimethylammonium tetrafluoroborate gave a 1 : 1 mixture of the expected iminium salt (9*Z*)-**3** together with the all-*E* isomer **3** (including traces of 13*Z* isomers). Almost the same isomer distribution was obtained when starting the synthetic sequence with the nitrile (9*Z*,13*Z*)-**5** instead. Here isomerisation prevented us from obtaining the targeted product (9*Z*,13*Z*)-**3**.

From the iminium salt product distributions, it is very clear that 9*Z*→9*E* and, in particular, 13*Z*→13*E* isomerisations occur readily. In consequence, the isolated products were in favour of the all-*E* isomer **3** (or at least ~50%), whatever aldehyde was chosen as precursor.

^{1}H NMR spectroscopy

The ^{1}H NMR chemical shifts of the locked retinal isomers are collected in Table 1; the atom numbering is depicted in Fig. 2. Significant downfield shifts are observed for the protons at C12 (H–C_{12}) and C15 (H–C_{15}) in the 13*Z*-isomers [(13*Z*)-**6** and (9*Z*,13*Z*)-**6**] relative to those in the 13*E*-isomers [**6** and (9*Z*)-**6**].

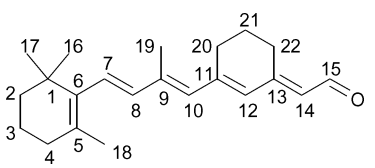

Fig. 2 Atom numbering; *cf.* Table 1.

Table 1 ^{1}H NMR chemical shifts (δ_H/ppm) of locked retinal derivatives in $CDCl_3$

Compd.	H–C_{22}	H–C_{21}	H–C_{20}	H–C_{19}	H–C_{18}	H–$C_{16/17}$	H–C_{15}	H–C_{14}	H–C_{12}	H–C_{10}	H–C_8	H–C_7	H–C_4	H–C_3	H–C_2
6	2.88	1.86	2.49	2.07	1.71	1.03	10.06	5.81	6.25	5.95	6.11	6.28	2.02	1.62	1.47
(9*Z*)-**6**	2.86	1.83	2.38	2.03	1.72	1.02	10.05	5.77	6.23	5.85	6.55	6.33	2.03	1.60	1.45
(13*Z*)-**6**	2.47	1.84	2.47	2.08	1.71	1.03	10.17	5.70	7.18	5.98	6.12	6.27	2.02	1.62	1.47
(9*Z*,13*Z*)-**6**	2.46	1.83	2.37	2.00	1.71	1.02	10.14	5.67	7.10	5.89	6.56	6.33	2.00	1.60	1.45

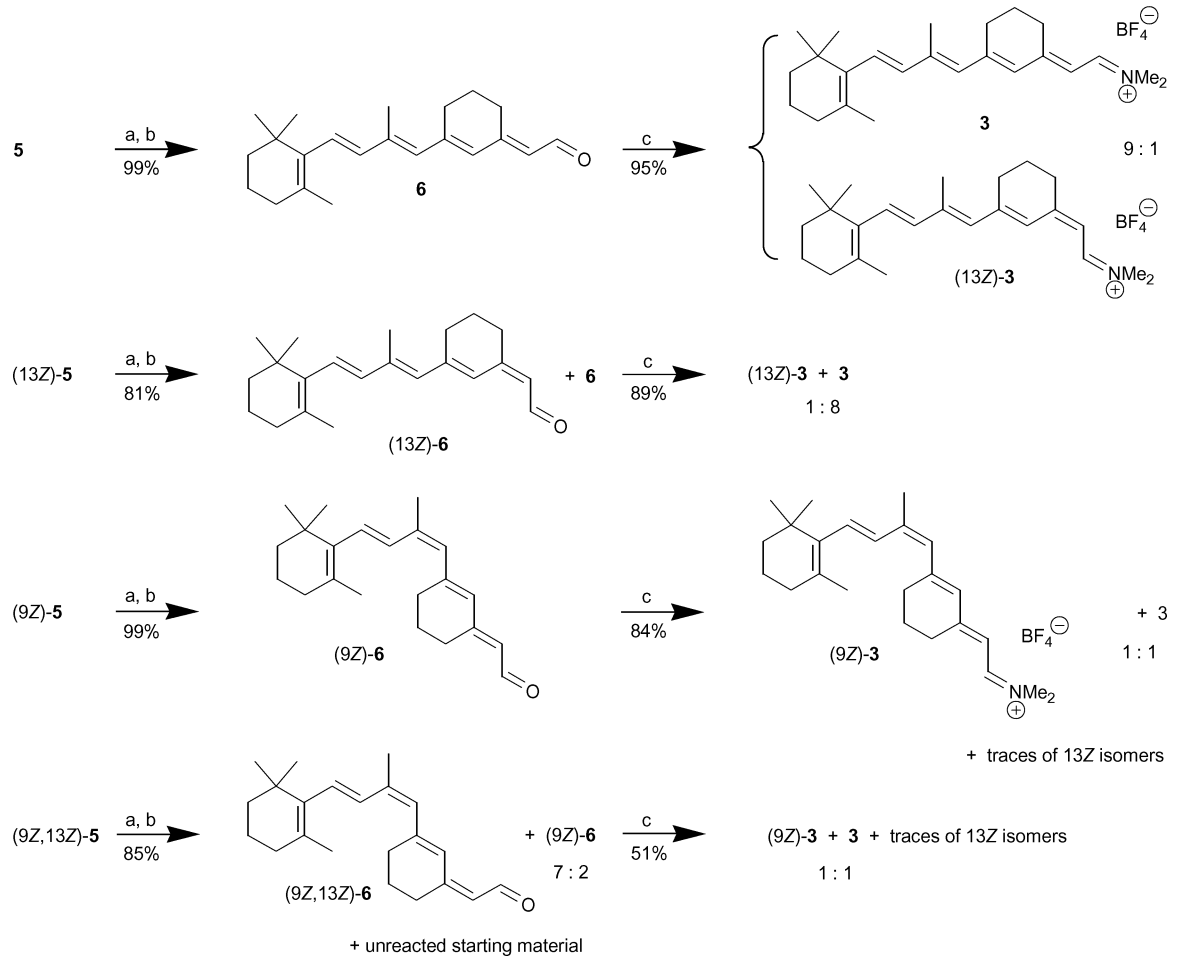

Scheme 2 *Reagents and conditions*: (a) DIBALH, pentane, −78 °C; (b) SiO_2, Et_2O, 0 °C; (c) $BF_4NH_2Me_2$, 4 Å sieves, EtOH, 0 °C.

In contrast, the protons at C14 and C22 are significantly upfield-shifted in the 13*Z*-isomers. The 9*Z*-isomers experience upfield shifts for the protons at C10, C19, and C20 relative to those in the 9*E*-isomers, while downfield shifts are observed for the protons at C7 and C8.

X-Ray crystallographic analysis

Single crystals of the nitriles (9*Z*)-**5** and (9*Z*,13*Z*)-**5** were grown from heptane by slow evaporation at *ca.* 5 °C. The solvent was allowed to completely evaporate since the crystals dissolve at room temperature. The X-ray crystal structures confirm the isomer designations and are revealed in Figs. 3 and 4. Both structures adopt the s-*cis* conformation at the "C8–C11" bond (defined according to crystal structure atom numbering). The conjugated section is non-planar for both molecules and can be separated in three intersecting planes defined by atoms C9, C8, C11

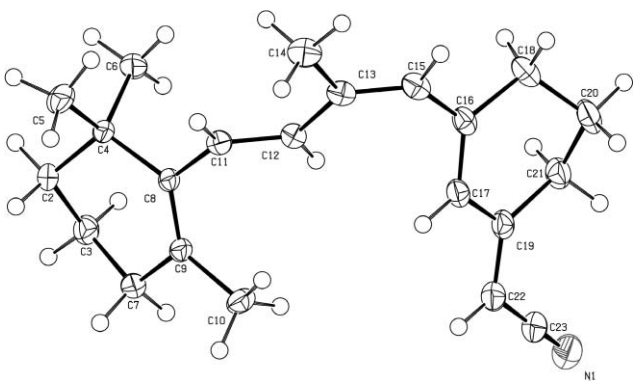

Fig. 3 X-ray crystal structure of (9*Z*)-**5**. Drawing made by ORTEP-II.[16] The atom ellipsoids are drawn at the 50% probability level.

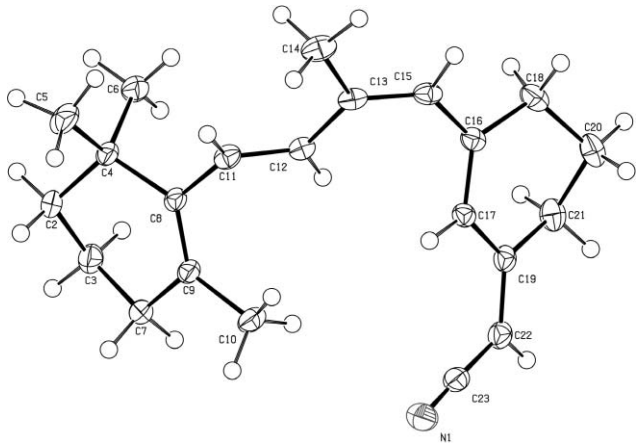

Fig. 4 X-ray crystal structure of (9*Z*,13*Z*)-**5**. Drawing made by ORTEP-II.[16] The atom ellipsoids are drawn at the 50% probability level.

(plane 1), C11, C12, C13, C15, C16 (plane 2) and C16, C17, C19, C22, C23 (plane 3). For (9*Z*)-**5**, planes 1 and 2 intersect at an angle of 48.6°, planes 2 and 3 at an angle of 46.5°, and planes 1 and 3 at an angle of 78.6°. For (9*Z*,13*Z*)-**5**, the corresponding angles are 44.4°, 51.7° and 82.9°.

Computational study

The locked derivatives **3**, (9*Z*)-**3**, (13*Z*)-**3** and (9*Z*,13*Z*)-**3** were subjected to semiempirical (PM3) geometry optimisations (in differently preselected s-*cis* and s-*trans* conformations), employing the Gaussion 03 program package.[17] The PM3 method was chosen for geometry optimisation since it was previously found to describe the structures of retinal Schiff bases well, whereas it largely underestimates rotational barriers.[18] Frequencies were calculated to verify that the calculated structures are local minima on the potential energy surface and to correct for zero-point kinetic energies. Density Functional Theory (DFT) single-point energies of the optimised structures were calculated at the B3LYP/6–31 + G(d) and B3LYP/6–311++G(2d,p) levels. Optimised structures and relative energies (at 0 K) are revealed in Fig. 5. The 6,7 s-*cis* conformer of the all-*E* isomer **10** was found to be 0.3–0.5 kcal mol^{-1} more stable than the s-*trans* conformer.[19] The conjugated section is almost planar in both conformers, not including, however, the cyclohexene double bond (C5–C6–C7–C8 torsional angle of *ca.* 42°). The conjugated sections of the 9*Z* and 13*Z* isomers in 10,11 s-*trans* or s-*cis* conformations deviate considerably from planarity, and these isomers are higher in energy than the all-*E* isomer. It is worth pointing out that the two

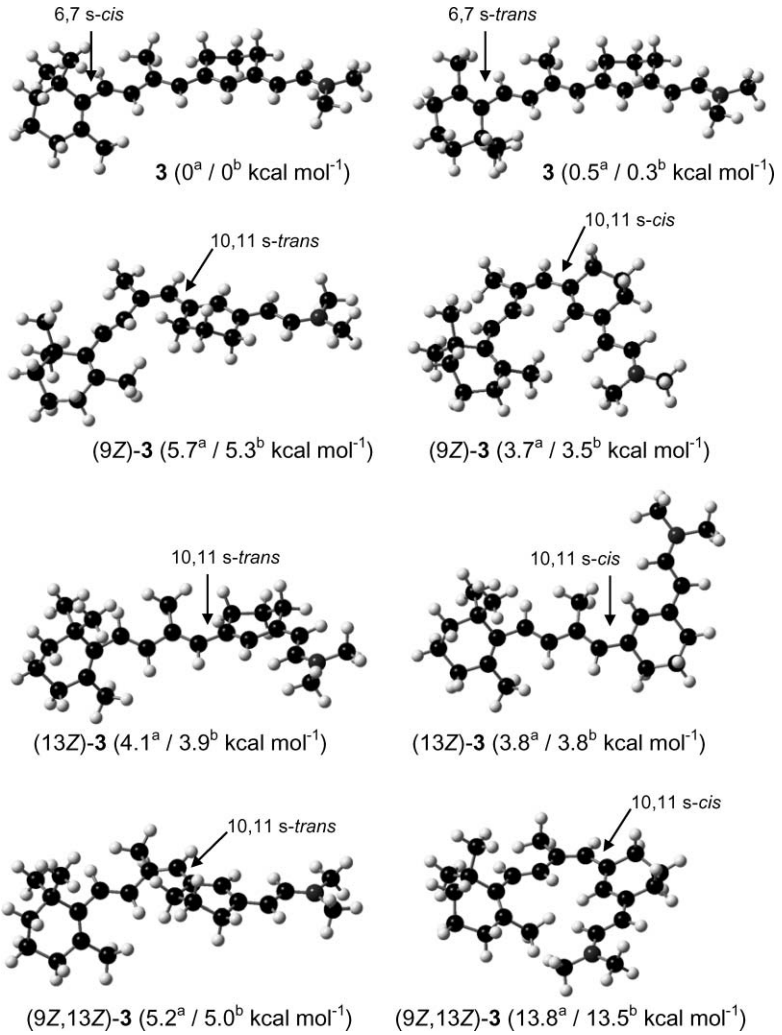

Fig. 5 PM3-optimised structures and relative energies calculated at the a) B3LYP/6–31 + G(d) and b) B3LYP/6–311++G(2d,p) level.

optimised conformations of the 9*Z*,13*Z* isomer are considerably energetic in view of the fact that this isomer could not be isolated in our attempted synthesis. The 10,11 s-*cis* conformation of both (9*Z*)- and (13*Z*)-**3** is more stable than the corresponding s-*trans* conformation, while the opposite is true for (9*Z*,13*Z*)-**3** where the 10,11 s-*cis* conformation enforces unfavourable steric interactions. These interactions are less severe for the nitrile (9*Z*,13*Z*)-**5** for which the 10,11 s-*cis* conformation is in fact more stable (by 2.1–2.2 kcal mol^{-1}) than the s-*trans* conformation. Indeed, the 10,11 s-*cis* conformation is adopted by (9*Z*,13*Z*)-**5** in the solid state according to the X-ray crystallographic analysis (*vide supra*).

Absorption spectroscopy

The longest wavelength absorption maxima for the nitrile and aldehyde isomers as well as for the iminium salts in different solvents are listed in Tables 2 and 3. Moreover, the gas phase absorption maxima (vertical transitions) previously measured for **1** and slightly modified data for **2** are included in the table,[11] together with the new gas phase data obtained for the locked cationic mimic **3** (including isomer impurities).

Despite the preference for non-planar structures of (9*Z*)-**3** and (13*Z*)-**3** as predicted from the calculational study, these isomers experience absorption maxima in solution close to that of the all-*E* isomer **3**, for which the linear chain is almost planar according to the calculations. Thus, all isomers absorb in the region λ_{max} 489–494 nm in CH_2Cl_2 as inferred from a careful comparison of the absorption spectra of the different isomer mixtures isolated. This region is only slightly blue-shifted relative to the maximum of iminium salt **2** (Fig. 6). A slightly more significant blue-shift is observed when comparing the related bacteriorhodopsins. Thus, Albeck *et al.*[15] incubated aldehyde **6** with bacteriorhodopsin and obtained pigments that absorbed at λ_{max} 556 nm, while the natural bacteriorhodopsin absorbs at λ_{max} 570 nm.

In the gas phase (*i.e.*, without an environment containing negative counter-ions), compound **3** exhibits two main absorption peaks at λ_{max} = 546 and 594 nm (Fig. 7). The peak at the longest wavelength is attributed to a vertical $S_0 \rightarrow S_1$ transition without significant vibrational excitation in the S_1 state. The energy

Table 2 Longest wavelength absorption maxima (λ_{max}/nm) of nitriles and aldehydes in solution

Compd.	Hexane	Compd.	Hexane	CH_2Cl_2
5	344	**6**	358 (356[a])	378
(9*Z*)-**5**	343	(9*Z*)-**6**	359	379
(13*Z*)-**5**	343	(13*Z*)-**6**	352 (350[a])	368
(9*Z*,13*Z*)-**5**	348	(9*Z*,13*Z*)-**6**	355	373
		all-*trans*-retinal	369	382

[a] Ref. [15].

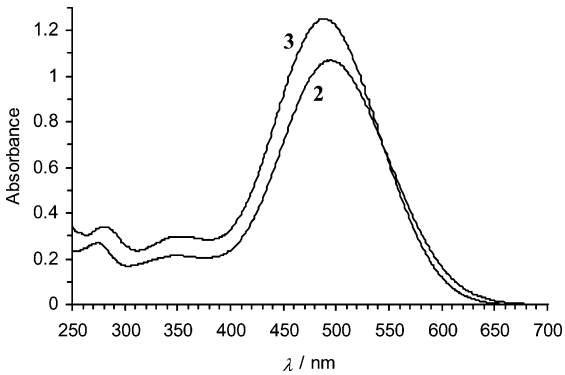

Fig. 6 Absorption spectra of **2** (2.8×10^{-5} M; all-*E*/13*Z* 7 : 1) and **3** (5.2×10^{-5} M; all-*E*/13*Z* 9 : 1) in CH_2Cl_2.

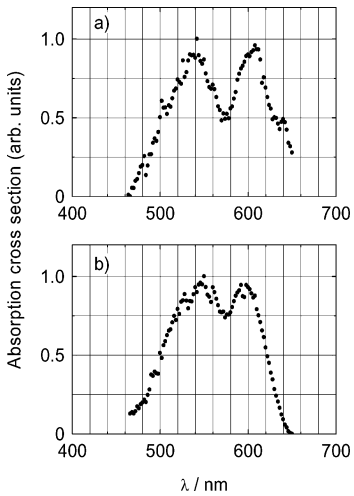

Fig. 7 Absorption spectra of a) **2** (all-*E*/13*Z* 7 : 1) and b) **3** (all-*E*/13*Z* 9 : 1) in the gas phase.

difference between the peaks corresponds to 1480 cm^{-1} which indicates that the structure at 546 nm may be related to C–C vibrations in the excited S_1 state. Thus, the calculated IR spectrum shows a strong absorption in this neighbourhood at 1410 cm^{-1} (value obtained after scaling with the PM3 scaling factor 0.9740). It should be noted that the transition to the second excited singlet state (S_2) is expected at a wavelength slightly below 400 nm.[20] In the gas phase, compound **2** exhibits two main absorption bands which peak at λ_{max} = 540 and 608 nm (Fig. 7). It appears that many vibrations may be excited in the $S_0 \rightarrow S_1$ transition; according to the spectrum, vibrational energies near 1400 and 3400 cm^{-1} may in particular be noticed.

The gas phase maximum (594 nm) of the locked chromophore **3** is slightly blue-shifted relative to that observed for chromophore **2** (608 nm), measured under exactly the same conditions. The small

Table 3 Longest wavelength absorption maxima (λ_{max}/nm) of retinylidene iminium compounds in solution and gas phase

	CH_2Cl_2	MeOH	Dioxane	DMSO	Gas phase
1	498	440			540sh, 610[a]
2	494	384, 450sh	448	447	540, 608[b]
3, (9*Z*)-**3**, (13*Z*)-**3**	489–494		442–446		546, 594

[a] Ref. [11]. [b] Slightly modified relative to those values published in ref. [11]; sh = shoulder.

blue-shift (14 nm) may be ascribed to a more limited conjugation in the locked chromophore. The intrinsic absorption maxima of compounds **2** and **3** are both red-shifted by 38 nm relative to those of the natural and artificial bacteriorhodopsins, respectively, which they are mimicking. Notably, all absorptions measured in solution (even in dichloromethane) are at higher energy than that of bacteriorhodopsin, and one would therefore have to be very careful in describing the influence of protein interactions by direct comparison with solvent values. The protein induces an increase, and not a decrease, in the energy of the transition relative to that of the isolated chromophore; this conclusion can only be drawn unambiguously from the gas phase investigation.

Finally, we would like to emphasise that the cationic mimics experience gas phase absorption spectra where the absorption in the blue region is very low. The large absorption blue-shift experienced in particular by blue cone pigments (λ_{max} 425 nm) is explained by a polar protein environment in proximity to the protonated iminium nitrogen as well as a closely situated negatively charged counter-ion.[2,21] These influences lead to a higher stabilisation of the ground-state relative to the excited state and hence a blue-shift. Similarly, a polar environment accounts for the high-energy absorption experienced in methanol solution (Table 3).

Conclusions

Although isomerically pure samples were not obtained on account of ready isomerisation, solution studies have revealed that isomeric 11-locked retinal Schiff bases exhibit almost identical absorption maxima, *i.e.*, structural deviations from planarity have a negligible influence. Along the same line, only a small blue-shift in absorption maximum is observed in the gas phase relative to a conformationally flexible, unlocked derivative. In our previous studies on unlocked retinal Schiff base derivatives,[11] the presence of two absorptions in the gas phase spectrum was somewhat puzzling. We have now confirmed that both these absorptions are indeed real and they are most likely the result of vibrational excitation in the S_1 state. Moreover, we can conclude that in the absence of protein interactions, the human eye would not detect light of wavelength shorter than 450 nm. In other words, we would not be able to perceive blue light.

Experimental

General methods

Chemicals were purchased from Aldrich and used as received. All reactions were carried out in the dark under an atmosphere of Ar or N_2. Thin-layer chromatography (TLC) was carried out using aluminium sheets pre-coated with silica gel 60F (Merck 5554). The plates were inspected under UV light. Dry column chromatography was carried out using silica gel 60 (Merck 15111, 0.015–0.40 mm). Flash column chromatography was carried out using silica gel 60 (Merck 9385, 0.040–0.063 mm). Melting points were measured on a Reichert melting point apparatus equipped with a microscope. ^{1}H NMR (300 MHz) and ^{13}C NMR (75 MHz) spectra were recorded on a Varian instrument, using the residual solvent as the internal standard. All chemical shifts are quoted on the δ scale (ppm), and all coupling constants (J) are expressed in Hz. Samples were prepared using $CDCl_3$ (Cambridge Isotope Labs) dried over molecular sieves (4 Å) and neutralised with basic Al_2O_3. Fast atom bombardment (FAB) mass spectra were obtained on a Jeol JMS-HX 110 Tandem Mass spectrometer in the positive ion mode using either 3-nitrobenzyl alcohol (NBA) or glycerol as matrix. Microanalyses were performed at the Microanalytical Laboratory at the Department of Chemistry, University of Copenhagen. Solution absorption spectra were recorded on a Shimadzu UV 1601PC instrument. Gas phase absorption spectra were obtained by applying the ELectrostatic Ion Storage ring in Aarhus (ELISA) as described elsewhere.[12]

Compounds 5 and (13*Z*)-5

NaH (60% in mineral oil, 130 mg, 3.25 mmol) was washed with dry *n*-pentane and taken up in dry DMF (60 mL) under N_2. Diethyl cyanomethylphosphonate (600 mg, 3.3 mmol) was added, and the solution was stirred for 15 min at rt followed by addition of isomerically pure **4** (800 mg, 2.8 mmol). After stirring at rt for 3 h, the reaction was quenched with sat. aqueous NH_4Cl (50 mL) followed by extraction with diethyl ether (3 × 50 mL). The combined organic phases were dried ($MgSO_4$) and evaporated *in vacuo*. Purification with repeated (3 ×) flash column chromatography (SiO_2, EtOAc–heptane 15 : 85 v/v) gave the two isomers **5** (360 mg, 42%) and (13*Z*)-**5** (227 mg, 26%) as yellow oils which solidified upon freezing. Compound **5**: $R_f = 0.53$ (EtOAc–heptane 3 : 17); δ_H (300 MHz, $CDCl_3$, 25 °C, 7.26 ppm) 6.25 (1 H, d, $J = 16.1$ Hz, C*H*), 6.18 (1 H, s, C*H*), 6.08 (1 H, d, $J = 16.1$ Hz, C*H*), 5.90 (1 H, s, C*H*), 5.00 (1 H, s, C*H*CN), 2.62 (2 H, t, $J =$ 6.2 Hz, CH_2), 2.42 (2 H, t, $J = 6.2$ Hz, CH_2), 2.01–1.99 (5 H, m, CH_3, CH_2), 1.81 (2 H, m, $J = 6.2$ Hz, CH_2), 1.70 (3 H, s, CH_3), 1.63–1.57 (2 H, m, CH_2), 1.48–1.44 (2 H, m, CH_2), 1.02 (6 H, s, CH_3); δ_C (75 MHz, $CDCl_3$, 25 °C, 77.0 ppm) 158.5, 147.4, 139.1, 138.1, 137.5, 131.0, 129.8, 128.9, 127.1, 118.3, 91.4, 39.5, 34.2, 33.0, 30.2, 28.9, 28.1, 22.2, 21.7, 19.2, 14.7; m/z (FAB$^+$, NBA) 308 (MH$^+$). Compound (13*Z*)-**5**: $R_f = 0.47$ (EtOAc–heptane 3 : 17); δ_H (300 MHz, $CDCl_3$, 25 °C, 7.26 ppm) 6.67 (1 H, s, C*H*), 6.26 (1 H, d, $J = 16.1$ Hz, C*H*), 6.10 (1 H, d, $J = 16.1$ Hz, C*H*), 5.95 (1 H, s, C*H*), 4.90 (1 H, s, C*H*CN), 2.44–2.38 (4 H, m, CH_2), 2.08 (1 H, s, CH_3), 2.01 (2 H, t, $J = 6.2$ Hz, CH_2), 1.78 (2 H, m, CH_2), 1.70 (3 H, s, CH_3), 1.61 (2 H, m, CH_2), 1.46 (2 H, m, CH_2), 1.02 (6 H, s, CH_3); δ_C (75 MHz, $CDCl_3$, 25 °C, 77.0 ppm) 158.0, 147.8, 139.6, 138.2, 137.5, 131.1, 129.8, 129.0, 124.9, 117.6, 90.1, 39.5, 34.2, 33.0, 30.6, 30.2, 28.9, 22.5, 21.7, 19.2, 14.7; m/z (HR-FAB$^+$, NBA) 308.2351 (MH$^+$, $C_{22}H_{30}N$ requires 308.2378).

Compounds (9*Z*)-5 and (9*Z*,13*Z*)-5

Compounds (9*Z*)-**5** (286 mg, 33%) and (9*Z*,13*Z*)-**5** (450 mg, 52%) were obtained as yellow solids in a similar way (with stirring for 18 h) from isomerically pure (9*Z*)-**4** (801 mg). Samples of both compounds were recrystallised from heptane. Compound (9*Z*,13*Z*)-**5**: m.p. 84.5–85.5 °C. $R_f = 0.48$ (EtOAc–heptane 3 : 17); δ_H (300 MHz, $CDCl_3$, 25 °C, 7.26 ppm) 6.58 (1 H, s, C*H*), 6.55 (1 H, d, $J = 16.4$ Hz, C*H*), 6.34 (1 H, d, $J = 16.4$ Hz, C*H*), 5.90 (1 H, s, C*H*), 4.90 (1 H, s, C*H*CN), 2.39 (4 H, m, CH_2), 2.09–2.01 (5 H, m, CH_2, CH_3), 1.82–1.71 (5 H, m, CH_2, CH_3), 1.61 (2 H, m, CH_2), 1.47 (2 H, m, CH_2), 1.04 (6 H, s, CH_3); δ_C (75 MHz, $CDCl_3$, 25 °C, 77.0 ppm) 157.8, 147.8, 138.4, 137.7, 131.1

(2 C-double intensity), 130.1, 129.5, 124.8, 117.4, 90.3, 39.6, 34.2, 33.1, 30.8, 30.4, 29.0, 22.5, 22.0, 21.7, 19.2; *m/z* (HR-FAB$^+$, glycerol) 308.2382 (MH^+, $C_{22}H_{30}N$ requires 308.2378). Compound (9*Z*)-**5**: m.p. 104–104.5 °C (Found: C, 85.81; H, 9.64; N, 4.52. $C_{22}H_{29}N$ (307.47) requires C, 85.94; H, 9.91; N, 4.56%). $R_f = 0.41$ (EtOAc–heptane 3 : 17); δ_H (300 MHz, $CDCl_3$, 25 °C, 7.26 ppm) 6.51 (1 H, d, $J = 16.2$ Hz, C*H*), 6.31 (1 H, d, $J = 16.2$ Hz, C*H*), 6.17 (1 H, s, C*H*), 5.82 (1 H, s, C*H*), 4.96 (1 H, s, C*H*CN), 2.62 (2 H, t, $J = 5.9$ Hz, CH_2), 2.33 (2 H, t, $J = 5.9$ Hz, CH_2), 2.06–1.99 (5 H, m, CH_2, CH_3), 1.80 (2 H, m, $J = 6.4$ Hz, CH_2), 1.71 (3 H, s, CH_3),1.62 (2 H, m, CH_2), 1.47 (2 H, m, CH_2), 1.02 (6 H, s, CH_3); δ_C (75 MHz, $CDCl_3$, 25 °C, 77.0 ppm) 158.5, 147.1, 138.3, 137.9, 131.4, 130.7, 130.0, 129.2, 127.0, 118.3, 91.5, 39.5, 34.2, 33.0, 30.3, 28.9, 28.2, 22.1, 22.0, 21.7, 19.1; *m/z* (FAB$^+$, glycerol) 308.

Compound 6

Isomerically pure **5** (234 mg, 0.76 mmol) was dissolved in dry *n*-pentane (50 mL) and cooled to −78 °C. DIBALH (1 M in hexanes, 2.4 mL, 2.4 mmol) was added, and the reaction mixture was allowed to stir at −78 °C for $2\frac{1}{2}$ h. Then diethyl ether (40 mL) and silica (5 g) were added, and after stirring overnight at 5 °C the reaction mixture was filtered through Celite and evaporated *in vacuo.* Purification by dry column chromatography (SiO_2, EtOAc–heptane 5%) gave **6** as a yellow oil (233 mg, 99%) with a trace of the 13*Z* isomer. $R_f = 0.27$ (EtOAc–heptane 3 : 17); δ_H (300 MHz, $CDCl_3$, 25 °C, 7.26 ppm) 10.06 (1 H, d, $J = 8.2$ Hz, C*H*), 6.28 (1 H, d, $J = 15.4$ Hz, C*H*), 6.25 (1 H, s, C*H*), 6.11 (1 H, d, $J = 15.4$ Hz, C*H*), 5.95 (1 H, s, C*H*), 5.81 (1 H, d, $J = 8.2$ Hz, C*H*), 2.88 (2 H, t, $J = 6.2$ Hz, CH_2), 2.49 (2 H, t, $J = 6.2$ Hz, CH_2), 2.07 (3 H, s, CH_3), 2.02 (2 H, m, CH_2), 1.86 (2 H, m, $J = 6.2$ Hz, CH_2), 1.71 (3 H, s, CH_3), 1.62 (2 H, m, CH_2), 1.47 (2 H, m, CH_2), 1.03 (6 H, s, CH_3); δ_C (75 MHz, $CDCl_3$, 25 °C, 77.0 ppm) 190.7, 157.2, 149.1, 139.5, 138.2, 137.6, 131.5, 130.2, 129.9, 129.1, 125.0, 39.5, 34.3, 33.0, 30.6, 28.9, 25.0, 22.4, 21.7, 19.2, 14.8; *m/z* (HR-FAB$^+$, NBA) 311.2355 (MH^+, $C_{22}H_{31}O$ requires 311.2375).

Compound (9*Z*)-6

Compound (9*Z*)-**6** was obtained as a thick, orange oil (256 mg, 99%) in a similar way from (9*Z*)-**5** (255 mg). Trace of isomer impurities. $R_f = 0.36$ (EtOAc–heptane 3 : 17); δ_H (300 MHz, $CDCl_3$, 25 °C, 7.26 ppm) 10.05 (1 H, d, $J = 8.3$ Hz, C*H*O), 6.55 (1 H, d, $J = 16.0$ Hz, C*H*), 6.33 (1 H, d, $J = 16.0$ Hz, C*H*), 6.23 (1 H, s, C*H*), 5.85 (1 H, s, C*H*), 5.77 (1 H, d, $J = 8.3$ Hz, C*H*), 2.86 (2 H, t, $J = 5.9$ Hz, CH_2), 2.38 (2 H, t, $J = 5.9$ Hz, CH_2), 2.03 (5 H, m, CH_2, CH_3), 1.83 (2 H, m, $J = 6.2$ Hz, CH_2), 1.72 (3 H, s, CH_3), 1.60 (2 H, m, CH_2), 1.45 (2 H, m, CH_2), 1.02 (6 H, s, CH_3); δ_C (75 MHz, $CDCl_3$, 25 °C, 77.0 ppm) 190.7, 157.0, 148.6, 138.5, 137.9 131.5, 130.9, 130.1, 129.8, 129.6, 125.1, 39.5, 34.2, 33.0, 30.7, 29.0, 25.1, 22.4, 22.0, 21.8, 19.2; *m/z* (HR-FAB$^+$, NBA) 311.2362 (MH^+, $C_{22}H_{31}O$ requires 311.2375).

Compound (13*Z*)-6

An isomeric mixture of compound (13*Z*)-**6** and **6** was obtained as a yellow oil (132 mg, 85%) in a similar way from (9*Z*)-**5** (154 mg). Dry column chromatography led to further isomerisation to **6**. Compound (13*Z*)-**6**: $R_f = 0.32$ (EtOAc–heptane 3 : 17); δ_H (300 MHz, $CDCl_3$, 25 °C, 7.26 ppm) 10.17 (1 H, d, $J = 8.2$ Hz, C*H*O), 7.18 (1 H, s, C*H*), 6.27 (1 H, d, $J = 15.8$ Hz, C*H*), 6.12 (1 H, d, $J = 15.8$ Hz, C*H*), 5.98 (1 H, s, C*H*), 5.70 (1 H, d, $J = 8.2$ Hz, C*H*), 2.47 (4 H, t, $J = 6.2$ Hz, CH_2), 2.08 (3 H, s, CH_3), 2.02 (2 H, t, $J = 6.2$ Hz, CH_2), 1.84 (2 H, m, $J = 6.2$ Hz, CH_2), 1.71 (3 H, s, CH_3), 1.62 (2 H, m, 2H, CH_2), 1.47 (2 H, m, CH_2), 1.03 (6 H, s, CH_3); δ_C (75 MHz, $CDCl_3$, 25 °C, 77.0 ppm) 189.6, 156.7, 148.6, 139.4, 138.2, 137.6, 131.7, 129.9, 129.1, 123.5, 122.7, 39.5, 34.3, 33.0, 32.1, 30.9, 28.9, 22.6, 21.7, 19.2, 14.8; *m/z* (HR-FAB$^+$, NBA) 311.2367 (MH^+, $C_{22}H_{31}O$ requires 311.2375).

Compound (9*Z*,13*Z*)-6

An isomeric mixture of (9*Z*,13*Z*)-**9** (66%) and (13*Z*)-**9** (19%) was obtained from (9*Z*,13*Z*)-**5** (together with unreacted starting material (15%)). Further purification was not possible due to isomerisation. Compound (9*Z*,13*Z*)-**6**: $R_f = 0.45$ (EtOAc–heptane 3 : 17)-isomerisation on plate; δ_H (300 MHz, $CDCl_3$, 25 °C, 7.26 ppm) 10.14 (1 H, d, $J = 8.3$ Hz, C*H*O), 7.10 (1 H, s, C*H*), 6.56 (1 H, d, $J = 15.8$ Hz, C*H*), 6.33 (1 H, d, $J = 15.8$ Hz, C*H*), 5.89 (1 H, s, C*H*), 5.67 (1 H, d, $J = 8.3$ Hz, C*H*), 2.46 (2 H, t, $J = 6.2$ Hz, CH_2), 2.37 (2 H, t, $J = 6.2$ Hz, CH_2), 2.00 (5 H, m, CH_2, CH_3), 1.83 (2 H, m, $J = 6.2$ Hz, CH_2), 1.71 (3 H, s, CH_3), 1.60 (2 H, m, CH_2), 1.45 (2 H, m, CH_2), 1.02 (6 H, s, CH_3); δ_C (75 MHz, $CDCl_3$, 25 °C, 77.0 ppm) 189.6, 156.7, 148.3, 138.3, 137.8, 131.3, 131.0, 130.2, 129.9, 123.6, 122.3, 39.5, 34.2, 33.0, 32.2, 31.0, 29.0, 22.5, 22.0, 21.7, 19.1; *m/z* (HR-FAB$^+$, NBA) 311.2368 (MH^+, $C_{22}H_{31}O$ requires 311.2375).

Compounds 3 and (13*Z*)-3

Aldehyde **6** (49 mg, 0.16 mmol) was dissolved in absolute ethanol at 0 °C (3 mL), whereupon dimethylammonium tetrafluoroborate (27 mg, 0.20 mmol) and 4 Å molecular sieves were added. The reaction mixture was allowed to stir carefully at 5 °C overnight, and then it was filtered and evaporated *in vacuo.* The deep red solid residue was dissolved in dry CH_2Cl_2, filtered and evaporated *in vacuo* followed by washing with dry *n*-pentane, which gave a mixture of the two isomers **3** and (13*Z*)-**3** (64 mg, 95%) in a 9 : 1 ratio. Compound **3**: δ_H (300 MHz, $CDCl_3$, 25 °C, 7.26 ppm) 8.53 (1 H, d, $J = 11.6$ Hz, C*H*N), 6.52 (1 H, s, C*H*), 6.43 (1 H, d, $J = 16.0$ Hz, C*H*), 6.16 (1 H, d, $J = 16.0$ Hz, C*H*), 6.14 (1 H, d, $J = 11.6$ Hz, C*H*CHN), 6.05 (1 H, s, C*H*), 3.66 (3 H, s, CH_3), 3.42 (3 H, s, CH_3), 2.84 (2 H, t, $J = 6.2$ Hz; CH_2), 2.60 (2 H, t, $J = 6.2$ Hz; CH_2), 2.14 (3 H, s, CH_3), 2.03 (2 H, m, CH_2), 1.88 (2 H, m, $J = 6.1$ Hz, CH_2), 1.71 (3 H, s, CH_3), 1.61 (2 H, m, CH_2), 1.47 (2 H, m, CH_2), 1.03 (6 H, s, CH_3); δ_C (75 MHz, $CDCl_3$, 25 °C, 77.0 ppm) 169.4, 163.0, 158.1, 144.7, 138.0, 137.5, 131.9, 131.5, 131.4, 130.8, 112.9, 48.8, 40.0, 39.5, 34.3, 33.2, 31.1, 28.9, 25.8, 22.2, 21.8, 19.1, 15.3; NOESY experiments confirmed structure; *m/z* (HR-FAB$^+$, NBA): 338.2842 ($[M\text{-}BF_4]^+$, $C_{24}H_{36}N$ requires 338.2848). Compound (13*Z*)-**3**: δ_H (300 MHz, $CDCl_3$, 25 °C, 7.26 ppm) – only a few characteristic signals can be assigned due to signal overlap: 8.67 (1 H, d, $J = 11.6$ Hz, C*H*N), 7.07 (1 H, s, C*H*), 3.38 (3 H, s, CH_3).

Other isomer mixtures of 3

Aldehydes (9*Z*)-**6**, (13*Z*)-**6** and (13*Z*)-**6**/**6** were converted in a similar way to isomer mixtures of **3**. An unequivocal assignment of ^{1}H NMR resonances of isomers other than **3** was not possible.

Table 4 X-Ray diffraction parameters and statistics of compounds (9*Z*)-**5** and (9*Z*,13*Z*)-**5**

	(9*Z*)-**5**	(9*Z*,13*Z*)-**5**
Empirical formula	$C_{22}H_{29}N$	$C_{22}H_{29}N$
M_r	307.46	307.46
T/K	122(2)	122(2)
λ/Å	0.71073	0.71073
Crystal system	Orthorhombic	Orthorhombic
Space group	$P2_12_12_1$	$P2_12_12_1$
a/Å	9.8840(16)	9.8070(8)
α/°	90.0	90.0
b/Å	11.7110(11)	11.7490(12)
β/°	90.0	90.0
c/Å	16.091(2)	16.027(2)
γ/°	90.0	90.0
V/Å^3	1862.6(4)	1846.7(4)
Z	4	4
ρ_{calc}/g cm^{-3}	1.096	1.106
$\mu_{MoK\alpha}$/mm^{-1}	0.062	0.063
F(000)	672	672
Crystal size/mm^3	0.72 × 0.36 × 0.18	0.59 × 0.49 × 0.37
θ range/°	2.15–32.98	2.15–35.01
Reflections collected	50833	52673
Unique data	6990 [$R_{int} = 0.0674$]	8043 [$R_{int} = 0.0449$]
Obsd data [$I > 2\sigma(I)$]	6132	7116
GOF on F^2	1.094	1.117
R indices (all data)	$R1 = 0.055$, $wR2 = 0.113$	$R1 = 0.055$, $wR2 = 0.109$
Larg.diff.peak/hole/e Å^{-3}	0.31/−0.19	0.36/−0.14

Crystal structure determination of compounds (9*Z*)-5 and (9*Z*,13*Z*)-5†

Intensity data for (9*Z*)-**5** and (9*Z*,13*Z*)-**5** were collected at 122 K on a Bruker-Nonius KappaCCD diffractometer equipped with an Oxford Cryostream unit. Data were reduced with EvalCCD,[22] the structures solved by direct methods using SIR97[23] and refined by least-squares against F^2 with SHELXL97[24] as incorporated in the maXus program.[25] For both structures all non-hydrogen atoms were anisotropically refined. All hydrogen atoms were found in subsequent difference Fourier maps and refined using a riding model. Experimental parameters and statistics are summarized in Table 4.

Acknowledgements

The Lundbeck Foundation and the Velux Foundation are gratefully acknowledged for supporting this project. Moreover, we acknowledge financial support from the Danish Natural Science Research Council (grants # 2111-04-0018 and 21-03-0330).

References

1 G. Wald, *Science*, 1968, **162**, 230–239.
2 G. G. Kochendoerfer, S. W. Lin, T. Sakmar and R. A. Mathies, *Trends Biochem. Sci.*, 1999, **24**, 300–305.
3 B. K. Fung and L. Stryer, *Proc. Natl. Acad. Sci.*, 1980, **77**, 2500–2504.
4 K. Palczewski, T. Kumasaka, T. Hori, C. A. Behnke, H. Motoshima, B. A. Fox, I. Le Trong, D. C. Teller, T. Okada, R. E. Stenkamp, M. Yamamoto and M. Miyano, *Science*, 2000, **289**, 739–745.
5 L. Stryer, *Biochemistry*, 2000, (Freeman, New York).
6 D. Oesterhelt and W. Stoeckenius, *Nature New Biol.*, 1971, **233**, 149–152.
7 D. Oesterhelt, *Angew. Chem., Int. Ed. Engl.*, 1976, **15**, 17–24; W. Stoeckenius, *Acc. Chem. Res.*, 1980, **13**, 337–344; U. Haupts, J. Tittor and D. Oesterhelt, *Ann. Rev. Biophys. Biomol. Struct.*, 1999, **28**, 367–369; J. K. Lanyi, *Nature*, 1995, **375**, 461–463.
8 R. S. Becker and K. Freedman, *J. Am. Chem. Soc.*, 1985, **107**, 1477–1485; K. A. Freedman and R. S. Becker, *J. Am. Chem. Soc.*, 1986, **108**, 1245–1251.
9 N. K. Nakanishi, V. Balogh-Nair, M. Arnaboldi, K. Tsujimoto and B. Honig, *J. Am. Chem. Soc.*, 1980, **102**, 7945–7947.
10 R. R. Birge, T. M. Cooper, A. F. Lawrence, M. B. Masthay, C. Vasilakis, C.-F. Zhang and R. Zidovetzki, *J. Am. Chem. Soc.*, 1989, **111**, 4063–4074.
11 L. H. Andersen, I. B. Nielsen, M. B. Kristensen, M. O. A. El Ghazaly, S. Haacke, M. B. Nielsen and M. Å. Petersen, *J. Am. Chem. Soc.*, 2005, **127**, 12347–12350.
12 S. P. Møller, *Nucl. Instrum. Methods Phys. Res., Sect. A*, 1997, **394**, 281–286; J. U. Andersen, P. Hvelplund, S. B. Nielsen, S. Tomita, H. Wahlgreen, S. P. Møller, U. V. Pedersen, J. S. Forster and T. J. D. Jørgensen, *Rev. Sci. Instrum.*, 2002, **73**, 1284–1287; L. H. Andersen, O. Heber and D. Zajfman, *J. Phys. B.: At., Mol. Opt. Phys.*, 2004, **37**, R57–R88; S. B. Nielsen, J. U. Andersen, P. Hvelplund, B. Liu and S. Tomita, *J. Phys. B.: At., Mol. Opt. Phys.*, 2004, **37**, R25–R56.
13 L. H. Andersen, H. Bluhme, S. Boyé, T. J. D. Jørgensen, H. Krogh, I. B. Nielsen, S. Brøndsted Nielsen and A. Svendsen, *Phys. Chem. Chem. Phys.*, 2004, **6**, 2617–2627.
14 L. H. Andersen, S. B. Nielsen and S. U. Pedersen, *Eur. Phys. J. D*, 2002, **20**, 597–600; I. B. Nielsen, S. Boyé-Peronne, M. O. A. El Ghazaly, M. B. Kristensen, S. B. Nielsen and L. H. Andersen, *Biophys. J.*, 2005, **89**, 2597–2604; S. Boyé, S. B. Nielsen, H. Krogh, I. B. Nielsen, U. V. Pedersen, A. F. Bell, X. He, P. J. Tonge and L. H. Andersen, *Phys. Chem. Chem. Phys.*, 2005, **5**, 3021–3026.
15 A. Albeck, N. Friedman, M. Sheves and M. Ottolenghi, *J. Am. Chem. Soc.*, 1986, **108**, 4614–4618.
16 C. K. Johnson, 1976, *ORTEP-II, A Fortran Thermal-Ellipsoid Plot Program. Report ORNL-5138*, Oak Ridge National Laboratory, Oak Ridge, Tennessee, USA.
17 M. J. Frisch, G. W. Trucks, H. B. Schlegel, G. E. Scuseria, M. A. Robb, J. R. Cheeseman, J. A. Montgomery, Jr., T. Vreven, K. N. Kudin, J. C. Burant, J. M. Millam, S. S. Iyengar, J. Tomasi, V. Barone, B. Mennucci, M. Cossi, G. Scalmani, N. Rega, G. A. Petersson, H. Nakatsuji, M. Hada, M. Ehara, K. Toyota, R. Fukuda, J. Hasegawa, M. Ishida, T. Nakajima, Y. Honda, O. Kitao, H. Nakai, M. Klene, X. Li, J. E. Knox, H. P. Hratchian, J. B. Cross, C. Adamo, J. Jaramillo,

† CCDC reference numbers 294256 and 294257. For crystallographic data in CIF or other electronic format see DOI: 10.1039/b600121a

R. Gomperts, R. E. Stratmann, O. Yazyev, A. J. Austin, R. Cammi, C. Pomelli, J. W. Ochterski, P. Y. Ayala, K. Morokuma, G. A. Voth, P. Salvador, J. J. Dannenberg, V. G. Zakrzewski, S. Dapprich, A. D. Daniels, M. C. Strain, O. Farkas, D. K. Malick, A. D. Rabuck, K. Raghavachari, J. B. Foresman, J. V. Ortiz, Q. Cui, A. G. Baboul, S. Clifford, J. Cioslowski, B. B. Stefanov, G. Liu, A. Liashenko, P. Piskorz, I. Komaromi, R. L. Martin, D. J. Fox, T. Keith, M. A. Al-Laham, C. Y. Peng, A. Nanayakkara, M. Challacombe, P. M. W. Gill, B. Johnson, W. Chen, M. W. Wong, C. Gonzalez and J. A. Pople, *Gaussian 03, Revision B.03*, Gaussian, Inc., Pittsburgh PA, 2003.

18 H. Zhoua, E. Tajkhorshida, T. Frauenheim, S. Suhai and M. Elstner, *Chem. Phys.*, 2002, **277**, 91–103.

19 The 6-s-*trans* conformation is adopted, however, for many retinylidene iminium salts in the solid state; see for example: S. Harbison, S. Smith, J. Pardoen, J. Courtin, J. Lugtenburg, J. Herzfeld, R. Mathies and R. G. Griffin, *Biochemistry*, 1985, **24**, 6955–6962; G. S. Harbison, P. P. J. Mulder, H. Pardoen, J. Lugtenburg, J. Herzfeld and R. G. Griffin, *J. Am. Chem. Soc.*, 1985, **107**, 4809–4816; G. R. Elia, R. F. Childs, J. F. Britten, D. S. C. Yang and B. D. Santarsiero, *Can. J. Chem.*, 1996, **74**, 591–601. Moreover, bacteriorhodopsin requires the 6-s-*trans* conformation: R. van der Steen, P. L. Biesheuvel, R. A. Mathies and J. Lugtenburg, *J. Am. Chem. Soc.*, 1986, **108**, 6410–6411.

20 I. B. Nielsen, L. Lammich and L. H. Andersen, *Phys. Rev. Lett.*, 2006, **96**, 018304.

21 For studies of the influence exerted by a charge in proximity to the retinal chromophore, see for example: ref. 9; M. G. Motto, M. Sheves, K. Tsujimoto, V. Balogh-Nair and K. Nakanishi, *J. Am. Chem. Soc.*, 1992, **114**, 7947–7949; A. Albeck, N. Livnah, H. Gottlieb and M. Sheves, *J. Am. Chem. Soc.*, 1992, **114**, 2400–2411.

22 A. J. M. Duisenberg, L. M. J. Kroon-Batenburg and A. M. M. Schreurs, *J. Appl. Crystallogr.*, 2003, **36**, 220–229.

23 A. Altomare, M. C. Burla, M. Camalli, G. L. Cascarano, C. Giacovazzo, A. Guagliardi, A. G. G. Moliterni and R. Spagna, *J. Appl. Crystallogr.*, 1999, **32**, 115–119.

24 G. M. Sheldrick, 1997, *SHELXL97. Program for the Refinement of Crystal Structures*, University of Göttingen, Germany.

25 S. Mackey, C. J. Gilmore, C. Edwards, N. Stewart and K. Shankland, 1999, *maXus. Computer Program for the Solution and Refinement of Crystal Structures*, Bruker Nonius, The Netherlands, Macscience, Japan & The University of Glasgow.

